

# Bandwidth Allocation and Resource Adjustment for Stability Enhancement in Complex Networks

K. Y. Henry Tsang and K.Y. Michael Wong

*Department of Physics, The Hong Kong University of Science and Technology, Clear Water Bay, Kowloon, Hong Kong*

(Dated: July 20, 2022)

We introduce the message passing algorithm and discrete Green's function to elucidate how resource fluctuations determine flow fluctuations in a network optimizing a global cost function. To enhance the robustness of the network against fluctuations, we develop the schemes of optimal bandwidth allocation in links and optimal resource adjustment in nodes. With the total bandwidth of the network are fixed, the approach of optimal bandwidth allocation is to increase the bandwidth in links such that the number of overloaded links or the amount of excess flows in networks under fluctuations can be minimized. Similarly, the approach of optimal resource adjustment is to minimize the number of overloaded links in networks under fluctuations with the total resource change in the network fixed. Compared with the conventional approach of proportionate bandwidth assignment or resource reduction, it is found that the optimized bandwidth allocation or resource adjustment can highly enhance the stability of the networks against fluctuations. The changes of loads and currents prescribed by the optimal bandwidth allocation and resource adjustment schemes are correlated with each other, except for some nodes that exhibit relay effects.

## I. INTRODUCTION

Stability of power grids is essential for the development of modern societies. Due to improving engineering technology over years, power grids become more reliable and stable in supplying electricity. However, widespread blackouts of different scales in power grids still occurred frequently [1] even with the investment of advanced technology. In spite of the fact that blackouts in large power grids are rare, they cause overwhelming economical and social losses [2]. As a result, it is crucial to study the cause of large blackouts and more importantly, how to enhance the stability of the networks. It is found that a large blackout is usually caused by a cascading failure which is triggered by a small local failure in the network [3, 4]. When there is a link failure in the network, the current originally flowing in that failed link will redistribute to other links in order to satisfy the demands of the users. Such a redistribution of current flows generally increases the load of other links because the current used to be flowing in that failed link has to go through other links. Links with such an increase in current flow have a higher load and may break down. Those new failed links can trigger further links to break down by the same reason and this process continues to spread and causes a large global failure. In general, cascading failures can also occur in other complex networks other than power grids. Thus, there is an increasing number of studies on cascading failures in complex networks [5–9]. To prevent losses caused by cascading failures in the network, methods of controlling cascades in complex networks have also been widely investigated [10–12].

Many network problems can be formulated as a flow optimization problem and thus, optimization of network flow problems is an important problem in science. The optimization of network flows was found to have wide applications in electric networks, transportation networks, communication networks [13, 14]. The network flow op-

timization problems are usually approached by finding a specific cost function to minimize. For example, the cost function may represent the power dissipation in electric network or time delays in communication networks. Traditionally, these optimization problems are approached by using graph theory and global optimization techniques, such as linear or quadratic programming [15]. Nevertheless, when the network size increases, global optimization becomes increasingly costly and infeasible. Interestingly, many large complex networks can be treated as disordered systems and methods from statistical mechanics of disordered systems are found to be useful in studying large complex networks [16]. For example, the cavity method originating from statistical mechanics [17, 18] was found to be computationally efficient and useful in studying network optimization problems. In this work, we also introduce two distributive methods, the message passing algorithm [14, 19] and chemical potential methods for calculating the current flows with a general cost function.

There are new challenges about the stability in power grid systems in recent years due to the introduction of renewable energy sources, such as wind power and solar power. Renewable energy usually has strong fluctuations, and such increasing deployment of renewable energy in power grids endanger the stability of the networks [20]. This is because power grids usually operate near their capacity limits. Flow fluctuations can cause the current flow to exceed the capacity of the transmission cables. Seeing that a small number of link failures can cause a large failure in the network, it can largely affect the stability of the network and it becomes important to study the flow fluctuations in the network [21].

Many networks used for resource transportation or communication have some capacity (or bandwidth, depends on network models) assigned to a node (a link) to withstand the flows through it. One common way to increase the robustness of the network is to increase the

capacities of nodes or bandwidths of links. Traditionally, the capacity layout used is the proportionate increase in initial loads [22–24]. However, it is found that the proportionate increase in capacities is not effective and costly to enhance the stability of the networks [22, 23]. Hence, there are studies about how to increase the robustness of the network by finding a better capacity layout [21, 25, 26]. From these studies, it is found that using a different capacity layout can largely increase the robustness of the networks. As fluctuations in the network can largely affect the stability of the network, there are studies in finding a better capacity layout against fluctuations [21]. Therefore, in this work, we study improved schemes of allocating bandwidths in the links of the network to prevent cascading failures caused by fluctuations. Usually, allocating bandwidths is more useful in the design stage of networks. In real time control, it is more practical to control the resources in the network. Therefore, we also study an optimal scheme of adjusting the resource in the network to enhance the stability of the network.

In Sec. II, we introduce the model for the networks and two methods of calculating the network flow, the cavity approach and discrete Green’s function approach will be described. The two methods are then used for predicting the variance of flow fluctuations given the information of resource fluctuations, verified by simulation results on some network structures in Sec. III. In Sec. IV, using the predicted variance of the flow fluctuations, we develop the optimized bandwidth allocation against fluctuations to increase the stability of the network. In Sec. V, we formulate an optimal resource adjustment scheme in the form of a constrained optimization problem to enhance the robustness of the network against fluctuations. The summary is presented in the final section.

## II. THE MIN-COST NETWORK FLOW MODEL

We begin with a typical resource allocation network model similar to [14]. Consider a network with  $N$  nodes and each node  $i$  is assigned with resource  $\Lambda_i$ . Positive and negative values of  $\Lambda_i$  indicate that node  $i$  has a supply and demand of resources respectively. Nodes with  $\Lambda_i = 0$  relay the current flows only. For simplicity, the network does not have excess resources (i.e.  $\sum_i \Lambda_i = 0$ ). Let  $y_{ij} \equiv -y_{ji}$  be the current flow from node  $j$  to node  $i$  and it has to satisfy the conservation of flows,

$$\Lambda_i + \sum_{j \in \partial i} y_{ij} = 0, \quad (1)$$

where  $\partial i$  is the set of neighbors of node  $i$ . Besides satisfying the flow conservation constraint, the current flows are required to minimize the total transportation cost in which the transportation cost along link  $(ij)$  is given by a general even function  $\phi(y_{ij})$ . In general, cost functions of form  $\phi(y_{ij}) = y_{ij}^r$  can be convex or concave functions of

$y_{ij}$  depending on the modeling purpose. To avoid congestion in network,  $r > 1$  is usually used as it will penalize overlaps of flows while  $r < 1$  is used when we want to encourage overlaps of flows [27, 28]. To find the optimal current flows that minimize  $E = \sum_{(ij)} \phi(y_{ij})$  subject to the constraint Eq. (1), we introduce two updating methods, the message-passing algorithm and the chemical potential method, to solve the flow optimization problem.

### A. Message-Passing

The message-passing algorithm is a distributive method for calculating the optimal flows. It is also known as the belief propagation or the cavity method in physics [18, 29]. The message-passing algorithm is known to be exact in graphs with tree structure and is a good approximation in large sparse networks. This is because the probability of finding loops of finite lengths is vanishing in large sparse networks such that the network itself can be approximated as locally tree-like. For real-valued flow variables, the algorithm is known to be exact in even when loops are present in the network structure if it converges [14, 30]. A more detailed analysis of the message-passing algorithm formulated in the network flow model can be found in [14]. For completeness of the paper, the main ideas and steps of message-passing algorithm are outlined as follows. To begin with, we assume the network is locally tree-like such that the correlations among the branches of trees can be neglected. The nodes are considered to be arranged in generations which can be thought of a node  $j$  having its neighbor node  $i$  as its ancestor and other neighbors as its descendants. Then node  $j$  is connected to an ancestor node  $i$  of the previous generation and  $|\partial j| - 1$  descendant nodes of the next generation. The cavity energy  $E_{j \rightarrow i}(y_{ij})$  is then given by

$$E_{j \rightarrow i}(y_{ij}) = \min_{\{\Lambda_j + \sum_{k \in \partial j \setminus i} y_{jk} = y_{ij}\}} \left( \sum_{k \in \partial j \setminus i} E_{k \rightarrow j}(y_{jk}) \right) + \phi(y_{ij}). \quad (2)$$

Let the two-parameter message sent from node  $j$  to  $i$  be

$$(A_{ij}, B_{ij}) = \left( \frac{\partial E_{j \rightarrow i}}{\partial y_{ij}}, \frac{\partial^2 E_{j \rightarrow i}}{\partial y_{ij}^2} \right). \quad (3)$$

The first and second derivatives of the optimal solution lead to the forward message

$$A_{ij} = \phi'(y_{ij}) - \mu_{ij}, \quad B_{ij} = \phi''(y_{ij}) + \frac{1}{\sum_{k \in \partial j \setminus i} B_{jk}^{-1}}, \quad (4)$$

where

$$\mu_{ij} = \frac{\Lambda_j - y_{ij} + \sum_{k \in \partial j \setminus i} (y_{jk} - B_{jk}^{-1} A_{jk})}{\sum_{k \in \partial j \setminus i} B_{jk}^{-1}}. \quad (5)$$

The whole network is obtained by merging the two trees and therefore, the current flows are given by

$$y_{ij} = \arg \min_{\{y\}} [E_{j \rightarrow i}(-y) + E_{i \rightarrow j}(y) - \phi(y)]. \quad (6)$$

Alternatively, one can calculate the optimal flows by computing the chemical potentials for each nodes. The Lagrangian for optimization is

$$L = \sum_{(ij)} \phi(y_{ij}) + \sum_i \mu_i \left( \Lambda_i + \sum_{j \in \partial i} y_{ij} \right), \quad (7)$$

where  $\mu_i$  is the Lagrange multiplier which can be interpreted as the chemical potential of node  $i$ . Optimizing  $L$  with respect to  $y_{ij}$ , one obtains the current flows as

$$y_{ij} = [\phi']^{-1}(\mu_j - \mu_i), \quad (8)$$

where  $\phi'$  is the derivative of  $\phi$  with respect to its argument. The chemical potential  $\mu_i$  is given by the zero of the equation given by

$$g_i(x) = \Lambda_i + \sum_{j \in \partial i} [\phi']^{-1}(\mu_j - x). \quad (9)$$

In this work, we focus the transportation cost as a quadratic function and the total cost function is given by

$$E = \sum_{(ij)} \frac{y_{ij}^2}{2}. \quad (10)$$

The quadratic cost function is chosen as it is minimized in electrical networks according to Thomson's principle [31] will be shown to be equivalent to power grid networks in the direct current (DC) approximation. Due to the quadratic nature of the cost function, we can approximate the cavity energy in the following form [14, 32]

$$E_{j \rightarrow i}(y_{ij}) = \frac{a_{ij}}{2} (y_{ij} - \tilde{y}_{ij})^2 + d_{ij}. \quad (11)$$

Inserting the functional form of Eq. (11) for the descendants into Eq. (2), and minimizing  $E_{j \rightarrow i}(y_{ij})$  with respect to  $y_{jk}$ , one can obtain the messages  $a_{ij}$  and  $\tilde{y}_{ij}$  as the functions of the messages of descendants

$$a_{ij} = 1 + \frac{1}{\sum_{k \in \partial j \setminus i} a_{jk}^{-1}}, \quad (12)$$

$$\tilde{y}_{ij} = \frac{\Lambda_j + \sum_{k \in \partial j \setminus i} \tilde{y}_{jk}}{1 + \sum_{k \in \partial j \setminus i} a_{jk}^{-1}}. \quad (13)$$

From Eq. (6), the current flow  $y_{ij}$  is obtained as

$$y_{ij} = \frac{a_{ij} \tilde{y}_{ij} - a_{ji} \tilde{y}_{ji}}{a_{ij} + a_{ji} - 1}. \quad (14)$$

For networks with quadratic cost functions, we simply update the messages by iterating Eq. (12) and Eq. (13) until they converge and use the results to obtain the optimal current by Eq. (14).

## B. Chemical Potential

In the chemical potential method, we make use of Eq. (9) for the quadratic cost function to obtain

$$\sum_j L_{ij} \mu_j = \Lambda_i, \quad (15)$$

where  $L$  is the Laplacian matrix

$$L = D - A. \quad (16)$$

In the above equation,  $D$  is the  $N \times N$  diagonal matrix with diagonal elements  $D_{ii}$  being the degree  $d_i$  of node  $i$ , and  $A$  is the adjacency matrix. In matrix notation, Eq. (15) is equivalent to

$$L\mu = \Lambda, \quad (17)$$

where  $\mu$  and  $\Lambda$  are the column vectors of the chemical potentials and resources respectively. The chemical potentials are obtained by inverting Eq. (17),

$$\mu = G\Lambda, \quad (18)$$

where  $G$  is the pseudoinverse of  $L$ , which is also known as the discrete Green's function [33]. Hence, from Eq. (8), the current is directly given by

$$y_{ij} = \sum_l (G_{jl} - G_{il}) \Lambda_l. \quad (19)$$

Although the discrete Green's functions are nonlocal, they can be calculated once during the initial stage and subsequent estimations can be calculated by linear products. This greatly simplifies the centralized algorithm.

## C. Power Grids

The above techniques can be applied to study power grids in the DC approximation. To see this, we consider the power flow along a link from node  $j$  to  $i$  given by a sine function of the phase angle difference between two nodes [34]

$$P_{ij} = \frac{|V_i| |V_j| \sin(\theta_j - \theta_i)}{x_{ij}}, \quad (20)$$

where  $x_{ij}$  is the reactance of the transmission link  $(ij)$ ,  $\theta_i$  is the phase angle and  $V_i$  is the voltage for node  $i$ . In the DC approximation, differences between the phase angles for each pair of neighboring nodes are small and we can approximate the power flow equation as

$$P_{ij} \approx \frac{\theta_j - \theta_i}{x_{ij}}, \quad (21)$$

where the voltage for each node is conventionally chosen to be  $|V_i| \approx 1$  with a suitable unit. Denote  $P_i$  as the

power generation (or consumption) in node  $i$ , then the total power flow in node  $i$  is given by

$$P_i + \sum_{j \in i} \frac{\theta_j - \theta_i}{x_{ij}} = 0. \quad (22)$$

From Eq. (9) and Eq. (21), we can view the chemical potentials as the phase angles for the nodes and having a unit reactance for each transmission link. Furthermore, the flow conservation equation is equivalent to the power flow equation in a node in which the power generation or consumption can be treated as the node's resource. Thus, networks using the quadratic cost function together with the flow conservation constraint can be treated as power grid networks in the DC approximation.

### III. INDUCED FLOW FLUCTUATIONS

In this section, we study the flow fluctuations induced by the fluctuations in resources. To begin with, we write the resource of node  $i$  as the sum of two components,

$$\Lambda_i = \Lambda_i^0 + \delta\Lambda_i, \quad (23)$$

where  $\Lambda_i^0$  is the the original resource without fluctuation and  $\delta\Lambda_i$  is the resource fluctuations. The current flows  $y_{ij}^0$  are the original current flows without fluctuation dependent on  $\Lambda_i^0$  and  $\delta y_{ij}$  are the flow fluctuations dependent on  $\delta\Lambda_i$ . For small fluctuations we can calculate the mean and variance of the flow fluctuations by using the message-passing algorithm or discrete Green's function developed in the previous section. For simplicity, we assume that the resource fluctuations are independent.  $\langle \delta\Lambda_i \rangle$  and  $\langle \delta\Lambda_i^2 \rangle$  of the resource fluctuations are assumed to be known and used in estimating the flow fluctuations.

In the framework of message-passing the fluctuations in current flows  $\delta y_{ij}$  can be obtained from Eqs. (13) and (14)

$$\delta\tilde{y}_{ij} = \frac{a_{ij} - 1}{a_{ij}} \left( \delta\Lambda_j + \sum_{k \in \partial j \setminus \{i\}} \delta\tilde{y}_{jk} \right), \quad (24)$$

$$\delta y_{ij} = \frac{a_{ij} \delta\tilde{y}_{ij} - a_{ji} \delta\tilde{y}_{ji}}{a_{ij} + a_{ji} - 1}. \quad (25)$$

For simplicity, we assume the mean of resource fluctuations is zero  $\langle \delta\Lambda_i \rangle = 0$ . From Eq. (24),  $\langle \delta\Lambda_i \rangle = 0$  always give  $\langle \delta\tilde{y}_{ij} \rangle = 0$  and hence  $\langle \delta y_{ij} \rangle = 0$ . To estimate the second moment  $\langle (\delta\tilde{y}_{ij})^2 \rangle$ , one can square both sides of Eq. (24) and take the average. We obtain

$$\langle \delta\tilde{y}_{ij}^2 \rangle \approx \left( \frac{a_{ij} - 1}{a_{ij}} \right)^2 \left( \langle \delta\Lambda_j^2 \rangle + \sum_{k \in \partial j \setminus \{i\}} \langle \delta\tilde{y}_{jk}^2 \rangle \right). \quad (26)$$

Note that the cross terms  $\langle \delta\tilde{y}_{jk_1} \delta\tilde{y}_{jk_2} \rangle$  are assumed to be zero for  $k_1 \neq k_2$ . This is because whenever the message-passing algorithm is applied, the network structure is assumed to be tree-like (or at least locally tree-like) and

therefore, links connected to the same node are treated as different branches of sub-trees which do not have paths connected to each other. This leads to the cross-terms being ignored. Similarly, one can obtain  $\langle (\delta y_{ij})^2 \rangle$  as

$$\langle \delta y_{ij}^2 \rangle \approx \frac{a_{ij}^2 \langle \delta\tilde{y}_{ij}^2 \rangle + a_{ji}^2 \langle \delta\tilde{y}_{ji}^2 \rangle}{(a_{ij} + a_{ji} - 1)^2}. \quad (27)$$

The cross term is again ignored due to the same reason. With Eq. (26) and Eq. (27), a set of iterative equations is obtained to estimate the flow fluctuations.

Another way to estimate the flow fluctuations is to use the discrete Green's function formulation. From Eq. (19), the fluctuations in current flows can be obtained by

$$\delta y_{ij} = \sum_l (G_{jl} - G_{il}) \delta\Lambda_l. \quad (28)$$

The mean  $\langle \delta y_{ij} \rangle$  is obtained by taking average of Eq. (28) and is equal to 0 as  $\langle \delta\Lambda_i \rangle = 0$ . The second moment  $\langle (\delta y_{ij})^2 \rangle$  is obtained by taking the squares and then averaging on both sides of Eq. (28)

$$\langle \delta y_{ij}^2 \rangle = \sum_k (G_{jk} - G_{ik})^2 \langle \delta\Lambda_k^2 \rangle. \quad (29)$$

We test the accuracy of both approaches by simulations in random (ER) networks and the IEEE Reliability Test System 96 (RTS 96) power network [35]. The ER network is constructed by  $N = 100$  nodes with the connecting probability  $p = 0.05$ . In the simulations, the resource fluctuations are randomly drawn from the Gaussian distribution with mean  $\langle \delta\Lambda_i \rangle = 0$  and variance  $\langle \delta\Lambda_i^2 \rangle = 1$ . Figure 1 shows the simulation results. In the simulations, the resource fluctuations are introduced at the same instant of time to each sample having the same network structure. Both estimation methods give a good agreement with the simulation results in ER networks. On the other hand, for the RTS 96 network, the discrete Green's functions give good estimates of the flow fluctuations whereas the message passing algorithm underestimates the fluctuations for some links. The main reason for the inaccurate estimation is that message passing assumes that the network structure is tree like and ignore the covariance term in the equation. However, some of the nodes are connected in loops and this can render the estimation inaccurate. Discrete Green's function approach does not make such an assumption and hence it gives a higher accuracy in such network structures.

### IV. OPTIMAL BANDWIDTH ALLOCATION

Estimates of flow fluctuations are useful in allocating bandwidths to links in networks handling fluctuating traffic. In practice, each link has a capacity which allows the maximum amount of current before it becomes overloaded. In communication networks, such capacities

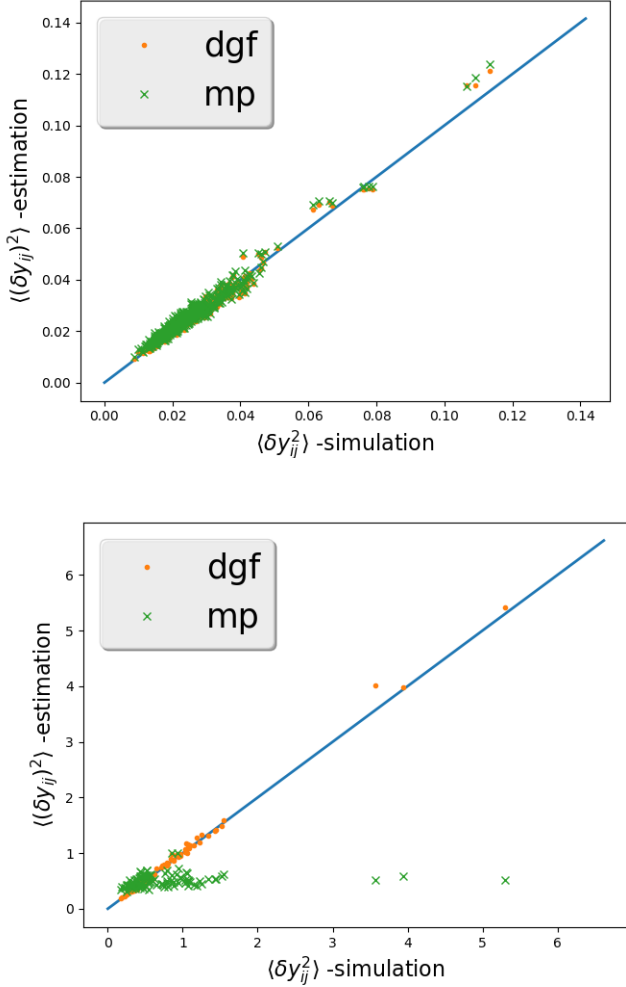


Figure 1. Comparison of the estimates of Eq. (29) (dgf) and Eq. (27) (mp) with simulation results (with 500 samples) in (a) ER networks and (b) the RTS 96 network.

usually refer to bandwidths and we generalize such terminology in this paper for convenience. Usually the bandwidth of a link is designed to be able to withstand the current flow of the network in the steady state with some tolerance. The reason for the tolerance is to prevent overload by a sudden increase or fluctuations in current flow. For simplicity, we decompose the bandwidth of a link into two parts,

$$L_{ij} = L_{ij}^0 + \Delta L_{ij}, \quad (30)$$

where  $L_{ij}^0 = |y_{ij}^0|$  and  $\Delta L_{ij} \geq 0$  represents the tolerance. The traditional bandwidth allocation is the proportionate bandwidth which has the form

$$L_{ij} = (1 + \epsilon)L_{ij}^0, \quad (31)$$

where  $\epsilon$  is the tolerance factor and  $\Delta L_{ij} = \epsilon L_{ij}^0$ . The proportionate bandwidth has been adopted to study the

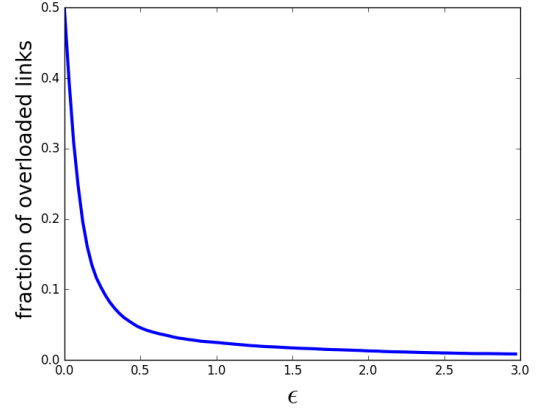


Figure 2. Simulation results of the fraction of overloaded links in the proportionate bandwidth allocation scheme as a function of the tolerance factor  $\epsilon$  for ER networks with average degree  $\approx 5$  and  $N = 100$ .

robustness of networks due to its simple proportionate form [22, 25]. In practice, increasing the bandwidths will increase the cost of constructing the network and hence,  $\epsilon$  is usually desired to be small. Therefore, for the purpose of designing a stable network, one is interested in increasing the robustness of the network by constraining  $\Delta L_{ij}$  with a given average tolerance factor (i.e.  $\sum_{(ij)} \Delta L_{ij} = \epsilon \sum_{(ij)} L_{ij}$ ). For a given tolerance factor, nevertheless, allocating bandwidth using the form of Eq. (31) is not effective against flow fluctuations.

To illustrate this, simulations in ER networks with the proportionate bandwidth allocation are used for investigation. In the simulation, we use the same setting for the ER network and the resource fluctuations as in Fig 1. When there are fluctuations in the current flows, the current may exceed the bandwidth and the link is considered overloaded when  $|y_{ij}| > L_{ij}$ . The fraction of overloaded links is used as a measurement of the robustness of the networks against fluctuations. From Fig. 2, it can be seen that the proportionate bandwidth allocation is not effective against fluctuations in the sense that there are still some overloaded links even when  $\epsilon$  is large (the existence of non-vanishing long tails). The main reason is the existence of links with small average current flow, yielding only small bandwidth increase even for large values of  $\epsilon$ .

To develop a better allocation of bandwidths to enhance the robustness of the network against fluctuations, we formulate an optimization problem subject to the constraint of fixed additional bandwidths. In this work, we focus on two objective functions, the expected number of overloaded links and the total amount of excess current in the network.

The functional form representing the expected number of overloaded links is determined by the probability distribution of the flow fluctuations. Considering  $\delta y_{ij}$  in the direction of increasing  $y_{ij}^0$ , it is sufficient to consider

the fraction of distribution with  $\delta y_{ij} > \Delta L_{ij}$  for distributions  $P_{ij}(\delta y_{ij})$  of the fluctuations. Thus, the expected number of overloaded links is given by

$$F = \sum_{(ij)} \int_{\Delta L_{ij}}^{\infty} P_{ij}(\delta y) d(\delta y). \quad (32)$$

$\Delta L_{ij}$  can then be evaluated such that it can minimize Eq. (32) subject to the constraints

$$\sum_{(ij)} \Delta L_{ij} = \epsilon \sum_{(ij)} L_{ij}^0 \text{ and } \Delta L_{ij} \geq 0. \quad (33)$$

The Lagrangian for optimization is given by

$$L = \sum_{(ij)} \int_{\Delta L_{ij}}^{\infty} P_{ij}(\delta y) d(\delta y) - \lambda \left( \sum_{(ij)} \Delta L_{ij} - \epsilon \sum_{(ij)} L_{ij}^0 \right) + \sum_{(ij)} \gamma_{ij} \Delta L_{ij},$$

where  $\lambda$  is the Lagrange multiplier and  $\gamma_{ij}$  is the Kuhn-Tucker multiplier. Assuming that  $P_{ij}(\delta y_{ij})$  are Gaussian distributions,  $\Delta L_{ij}$  that can minimize the total number of overloaded links is given by

$$\Delta L_{ij} = \begin{cases} 0, & \text{if } \langle (\delta y_{ij})^2 \rangle \geq 1/(2\pi\lambda^2), \\ \sqrt{\langle (\delta y_{ij})^2 \rangle} \left[ 2 \ln \left( \frac{1}{\lambda \sqrt{2\pi \langle (\delta y_{ij})^2 \rangle}} \right) \right]^{\frac{1}{2}}, & \text{otherwise.} \end{cases} \quad (34)$$

where  $\lambda$  is determined by the constraint Eq. (33). The conditional form of Eq. (34) is due to Kuhn-Tucker condition. For small given total cost, resources are allocated to those links with small flow fluctuations,  $\sqrt{\langle \delta y_{ij}^2 \rangle} < 1/2\pi\lambda$  (unlike the proportionate bandwidth allocation scheme which allocates the bandwidth resources to every links independent of the magnitude of flow fluctuations). When the tolerance factor  $\epsilon$  is increased, the non-linearity of Eq. (34) tends to distribute more bandwidth resources to links with moderate flow fluctuations to save the majority of links. Figure 3 illustrates the fraction of unchanged links ( $\Delta L_{ij} = 0$ ) as a function of the total cost in a random network with fixed connectivity  $d_i = 3$ . The variance of resource fluctuations is set to  $\langle \delta \Lambda_i^2 \rangle = k \langle \Lambda_i^2 \rangle$ . It shows that when  $k$  increases, the network requires higher tolerance to reduce the number of unchanged links.

However, the criterion of minimizing the expected number of overloaded links saves the additional bandwidths by focusing on the links with small fluctuations, whereas it allows those links with large fluctuations to be heavily overloaded. In practice, this may lead to a huge degradation of the quality of network service. Therefore, alternative cost functions should be considered.

An alternative cost function for the robustness of the network is the expected amount of excess current flows.

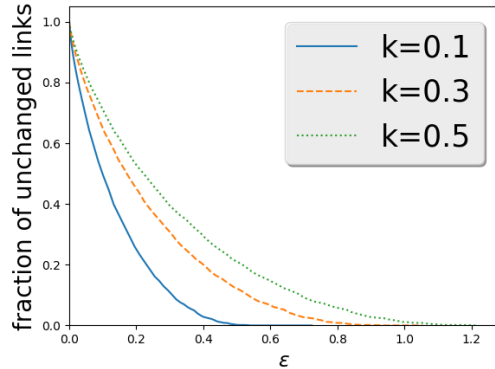


Figure 3. Dependence of the fraction of unchanged links on the tolerance factor  $\epsilon$  for different fluctuation magnitudes.

Excess current flow is defined as the amount of current flow exceeding the bandwidth

$$I_{ij} = \max(|\delta y_{ij}| - \Delta L_{ij}, 0). \quad (35)$$

Hence, the function measuring the total excess current flow in the network can be obtained as

$$F = \sum_{(ij)} \int_{\Delta L_{ij}}^{\infty} (\delta y - \Delta L_{ij}) P_{ij}(\delta y) d(\delta y) \quad (36)$$

Minimizing Eq. (36) subject to the total cost constraint as Eq. (33). One can obtain

$$\Delta L_{ij} = \epsilon' \sqrt{\langle (\delta y_{ij})^2 \rangle} \quad (37)$$

where  $\epsilon'$  is a function of the Lagrange multiplier and can be calculated by substituting  $\Delta L_{ij}$  into Eq. (33). Unlike the bandwidth allocation scheme that minimizes the expected number of overload link, Eq. (37) tends to distribute the bandwidth resources according to the flow fluctuations in the links. In fact, the form of Eq. (37) is similar to Eq. (31) where  $L_{ij}^0$  is replaced by  $\sqrt{\langle (\delta y_{ij})^2 \rangle}$ .

We compare the performances of the bandwidth allocation schemes by simulations in the RTS 96 network. In the simulations, the resource  $\Lambda_i^0$  for node  $i$  is picked from the Gaussian distribution with mean 0 and standard deviation 10. The resource fluctuations  $\delta \Lambda_i$  follows the Gaussian distributions with means 0 and variances  $0.09(\Lambda_i^0)^2$ . As expected, *minlink* has the least fraction of overloaded links while *minflow* has the least amount of excess current under flow fluctuations. Moreover, both *minlink* and *minflow* are able to completely protect the network with a smaller amount of total cost when compared with the proportionate bandwidth allocation scheme. Recall from Fig. 2, when the network uses the proportionate bandwidth allocation scheme, the total fraction of overloaded links in the network do not converge to zero even up to  $\epsilon \sim 3$ .

We also consider the allocation of bandwidths in randomly connected dilute networks with fixed connectivity  $K$  in Appendix. In these networks exact results

can be obtained using the cavity method. The currents have Gaussian distributions for Gaussian resource fluctuations. The proportionate allocation scheme yields an average excess current scaling as  $\epsilon^{-1}$  in the limit of large  $\epsilon$ . This behavior of convergence to zero is much weaker than the Gaussian tail convergence in the *minlink* and *minflow* schemes. Furthermore, *minlink* and *minflow* achieve this objective using a relatively small tolerance factor (and hence a small amount of investment cost) as compared with the proportionate bandwidth allocation scheme. As the derivation of *minlink* and *minflow* does not require assumptions on the particular structure or size of the network, *minlink* and *minflow* can work well for all network structures (and sizes).

From the figure showing the excess current flow in the network, there exist some points with discontinuous slope in the curve of *minlink*. The discontinuities come from the discontinuity in  $\Delta L_{ij}$  as derived in Eq. (34). Note that when the tolerance factor  $\epsilon$  increases,  $\mu$  increases as well. When  $\mu$  remains less than  $\sqrt{2\pi\langle\delta y_{ij}^2\rangle}$  of a link ( $ij$ ), its bandwidth decreases continuously with increasing  $\mu$ , but when  $\mu$  exceeds  $\sqrt{2\pi\langle\delta y_{ij}^2\rangle}$ , the bandwidth vanishes for all higher values of  $\mu$ . This results in a discontinuity of the slope in the curve *minlink* in Fig. 4(b) of the average excess current.

## V. OPTIMAL RESOURCE ADJUSTMENT

In the previous section, we study how to enhance the robustness of the network against fluctuations through increasing the total bandwidth. However, such an approach is usually more useful in network design. For real-time control, it is more practical to adjust the resources in nodes such as the implementation of load shedding in power engineering [36]. In dynamic control, usually only short-term predictions of fluctuations of power supply and demand in the form of probabilistic distributions are available. Therefore in this section, we study how to optimally adjust the resources in the nodes to increase the stability of the network given the probabilistic information of the fluctuations.

We begin by writing the resource  $\Lambda_i$  as

$$\Lambda_i = \Lambda_i^0 + \delta\Lambda_i + \pi_i, \quad (38)$$

where  $\Lambda_i^0$  is the original resource,  $\delta\Lambda_i$  is the resource fluctuations and  $\pi_i$  is the controllable component. For a power grid, one can treat the controllable component as the controllable power sources such as the power generated from natural gas or the load to be shed. When there are fluctuations in the resources, the induced flow fluctuations can cause overload in links and we consider link ( $ij$ ) to be overloaded when  $|y_{ij}| > L_{ij}$  as in the previous section. For simplicity, we set  $L_{ij} = |y_{ij}^0|$  in this section. With the introduction of  $\pi_i$ , the current flow  $y_{ij}$  can be written as

$$y_{ij} = y_{ij}^0 + \delta y_{ij} + z_{ij}, \quad (39)$$

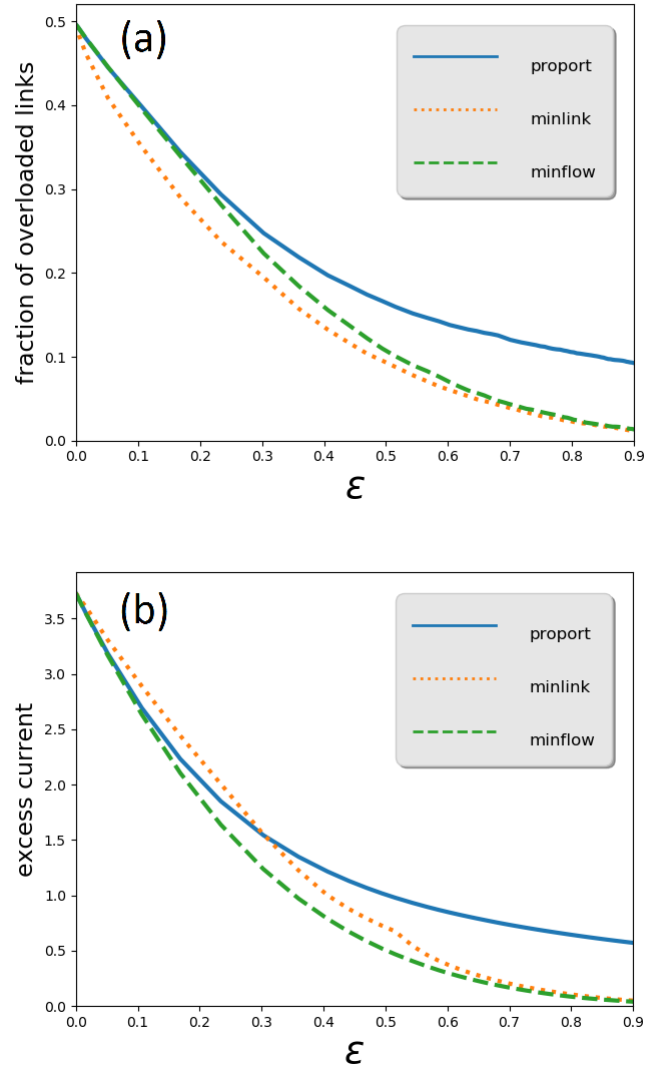


Figure 4. Simulation results of (a) the fraction of overloaded links and (b) the amount of excess current per link, in units of  $\langle\delta\Lambda^2\rangle$ , for the bandwidth allocation schemes in the RTS network as a function of the tolerance factor  $\epsilon$ . 100 samples of supply and demand are generated from the resource distribution. For simplicity, *proport*, *minlink* and *minflow* corresponds to the proportionate bandwidth allocation scheme, minimizing the expected number of overloaded links, and minimizing the expected amount of excess flows respectively.

where  $z_{ij} = \sum_l (G_{jl} - G_{il})\pi_l$ . Hence, with a proper value of  $\pi_i$ , the current flow can be reduced and our objective is to find the optimal  $\pi_i$  such that the total number of overloaded links is minimized. Suppose the resource fluctuations follow the Gaussian distribution, then the flow fluctuations will also follow the Gaussian distribution and

the objective function to be minimized is given by

$$\begin{aligned}
 F &= \frac{1}{E} \sum_{(ij)} \int_{L_{ij} - \text{sgn}(y_{ij}^0)(y_{ij}^0 + z_{ij})}^{\infty} P_{ij}(\delta y) d(\delta y) \\
 &= \frac{1}{2E} \sum_{(ij)} \text{erfc} \left( \frac{\text{sgn}(-y_{ij}^0) z_{ij}}{\sqrt{2\langle \delta y_{ij}^2 \rangle}} \right)
 \end{aligned} \tag{40}$$

where  $E$  is the total number of links. To have a practical resource adjustment, we introduce constraints to restrict the value of  $\pi_i$ . As there are no excess resources in the network, the sum of  $\pi_i$  have to be equal to zero (i.e.  $\sum_i \pi_i = 0$ ). Moreover, to have a fair comparison between different adjustment schemes, we introduce an additional constraint to restrict the total amount of changes in the resources,  $\sum_i |\pi_i| = c \sum_i |\Lambda_i^0|$ , where  $c$  is a parameter to control the total amount of changes. In fact, one can view  $c$  as the mean ratio to be changed in the resource for each node. Furthermore, we also restrict  $\pi_i$  to reduce the value of  $\Lambda_i^0$  (i.e.  $\text{sgn}(\Lambda_i^0)\pi_i \leq 0$ ) and that the changes do not reverse the nature of supply and demand of the nodes (i.e.  $-\text{sgn}(\Lambda_i^0)(\pi_i + \Lambda_i^0) \leq 0$ ). Combining all the constraints, we propose an optimal resource adjustment scheme by solving the following constrained optimization problem,

$$\begin{aligned}
 &\text{minimize}_{\{\pi_i\}} \quad \frac{1}{2E} \sum_{(ij)} \text{erfc} \left( \frac{\text{sgn}(-y_{ij}^0) z_{ij}}{\sqrt{2\langle \delta y_{ij}^2 \rangle}} \right), \\
 &\text{subject to} \quad \sum_i |\pi_i| = c \sum_i |\Lambda_i^0|, \\
 &\quad \quad \quad \sum_i \pi_i = 0, \\
 &\quad \quad \quad \text{sgn}(\Lambda_i^0)\pi_i \leq 0, \\
 &\quad \quad \quad -\text{sgn}(\Lambda_i^0)(\Lambda_i^0 + \pi_i) \leq 0.
 \end{aligned}$$

Since there is no analytical solution for the above optimization problem, one has to solve it numerically. Since the equality and inequality constraints are linear in the control variables  $\pi_i$ , it can be solved using the barrier methods [37]. For comparison in the RTS 96 network, we introduce the proportionate reduction scheme  $\pi_i^{prop} = -c(\Lambda_i^0)$  which proportionately reduces the current flow in the network.  $\Lambda_i^0$  follows a Gaussian distribution with mean equal to 0 and variance equal to 1 with the fluctuation  $\delta\Lambda_i$  following a Gaussian distribution with mean equal to 0 and variance equal to  $0.1(\Lambda_i^0)^2$  independently. Figure 5 shows that in the optimal adjustment scheme, the network has a much higher stability compared with the proportionate reduction.

Similar to the optimal bandwidth allocation scheme, the current reduction of the links in the optimal resource adjustment scheme is correlated with the strength of the flow fluctuations. In fact, links that are given larger bandwidths in the optimal bandwidth allocation scheme will usually experience a larger reduction in current flow

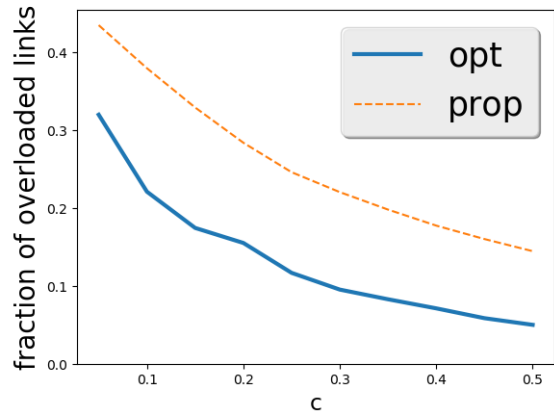


Figure 5. Simulation results of the fraction of overloaded links in the RTS network averaged over 100 samples as a function of the load-shedding ratio  $c$ .

according to the optimal resource adjustment scheme. From Fig. 6(a), one can see that those links having high current reduction in the resource adjustment scheme usually have a larger bandwidth allocated according to Eq. (37). For each value of rescaled fluctuation  $\sqrt{\langle \delta y_{ij}^2 \rangle} / |y_{ij}^0|$ , we compute the Pearson correlation coefficient between  $|z_{ij} / y_{ij}^0|$  and  $\sqrt{\langle \delta y_{ij}^2 \rangle} / |y_{ij}^0|$  in the range spanned from its value down to 0. Figure 6(b) shows that the correlation is positive.

We further compare the behaviors of the nodes under the optimal resource adjustment and bandwidth allocation schemes. Figure 7 shows the resource adjustment  $|\pi_i|$  against the total flow fluctuation  $\sqrt{\sum_{j \in \partial i} \langle \delta y_{ij}^2 \rangle}$  through node  $i$  in the RTS 96 network. From the figure, one can see that most nodes connected with links having large flow fluctuations require a larger reduction in resources. However, there are also considerable number of nodes having large flow fluctuations that do not have any changes in resources  $\pi_i = 0$ . In fact, those nodes can be viewed as nodes used for relaying the 'reduction' of current flow  $z_{ij}$ . Since those nodes are connected with links having large flow fluctuations, their connected links require a larger reduction in current flow such that the overload probability can be minimized. To satisfy the constraints in the optimization problem, some nodes are therefore used for relaying the flow reduction without themselves participating in load reduction. Usually, those nodes are connected with nodes that have a large reduction in resources. As an illustration, Fig. 8 shows the RTS 96 network with the same parameter setting as Fig. 5 with  $c = 0.3$  in which nodes with no change in resources are often connected with nodes having large changes in resources as shown in nodes a and b of Fig. 8.



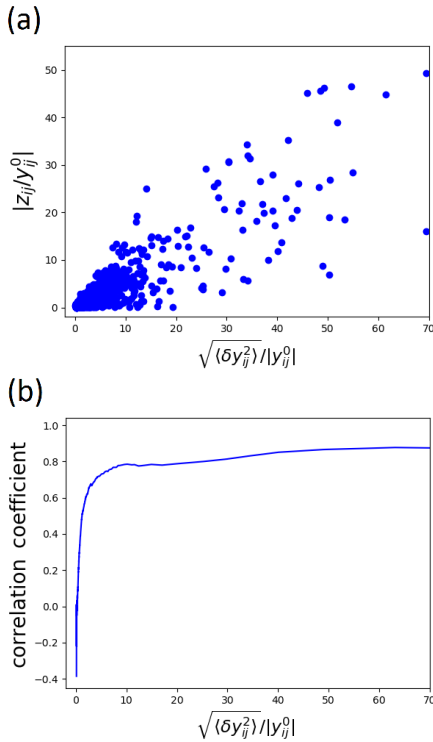


Figure 6. Comparison of the link behaviors in the optimal bandwidth allocation and resource adjustment schemes. We have used 30 samples of ER network with  $N = 100$  and  $p = 0.05$ . The resources and resource fluctuations have the same setting as in Fig. 5. (a)  $|z_{ij}/y_{ij}^0|$  versus  $\sqrt{\langle \delta y_{ij}^2 \rangle / |y_{ij}^0|}$  with  $c = 0.3$ . (b) Pearson correlation coefficient versus  $\sqrt{\langle \delta y_{ij}^2 \rangle / |y_{ij}^0|}$ .

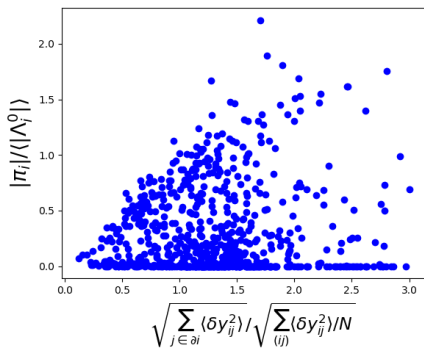


Figure 7. Comparison of the node behaviors in the optimal resource adjustment scheme (in terms of the rescaled resource adjustment  $|\pi_i| / \langle \Lambda_i^0 \rangle$ ) and the optimal bandwidth allocation scheme (in terms of the rescaled bandwidth adjustment  $\sqrt{\sum_{j \in \partial i} \langle \delta y_{ij}^2 \rangle} / \sqrt{\sum_{(ij)} \langle \delta y_{ij}^2 \rangle / N}$ ). The network and parameter setting are the same as Fig. 5 with  $c = 0.3$  (30 samples).

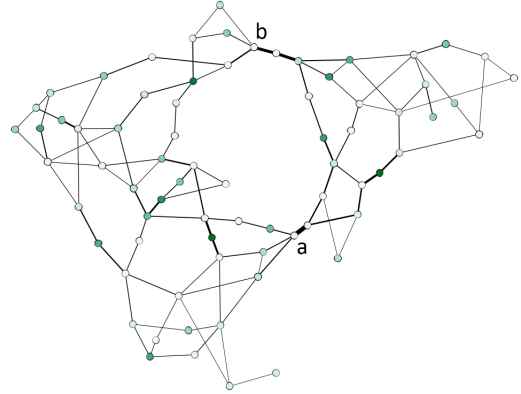


Figure 8. Illustration of the relay effect in the RTS 96 network with the same parameter setting as Fig. 5 [as mentioned in the text]. The darker the color of the node, the larger the changes  $|\pi_i|$ . The thickness of the edge represents the strength of the flow fluctuations  $\langle \delta y_{ij}^2 \rangle$ .

## VI. CONCLUSION

We have formulated the message-passing algorithm and chemical potential methods for finding the current flows in the transportation network with a general cost function. The methods can be applied to optimize stability in transportation networks and also power grids in the DC approximation. With the message-passing algorithm and the discrete Green's functions, one can estimate the mean and variance of the flow fluctuations induced by the resource fluctuations. From the simulation results, it is found that the estimations of flow fluctuations using the message-passing algorithm relies heavily on the locally tree-like structure of the networks. As the method of discrete Green's functions does not have any assumption on the network structures, the simulation results show that it gives more accurate results on different network structures. To improve the accuracy of the message-passing algorithm in estimating the variance of the flow fluctuations, one may need to improve the algorithm by considering loops in loopy graphs as in generalized belief propagation [38].

We have also shown that using the traditional proportionate bandwidth allocation cannot effectively increase the robustness of the networks against fluctuations. To properly allocate the bandwidths, we developed the optimal bandwidth allocation schemes that can minimize the total number of overloaded links or total excess current in the networks under fluctuations. Both simulation results in complex networks and analytical results in dilute networks show that the optimized methods of allocating bandwidth can effectively enhance the stability of the networks against fluctuations compared with the proportionate bandwidth allocation. Moreover, we developed a

scheme to optimally adjust the resources in the network such that it can minimize the total number of overloaded links under fluctuations. Simulation results show that using the proposed resource adjustment scheme can have a better performance than the proportionate resource reduction. Furthermore, we found that there is a close correlation between the optimal bandwidth allocation and resource adjustment schemes. The former assigns more bandwidths to links with large flow fluctuations while the latter reduces more current flow along them. Exceptions are some nodes connected to highly fluctuating links that relay their fluctuations to other links without their own participation in resource adjustments.

### ACKNOWLEDGMENTS

This work is supported by grants from the Research Grants Council of Hong Kong (grant numbers 16322616 and 16306817).

### APPENDIX

Using the cavity method, we will analytically show that the optimal bandwidth allocation schemes outperform the proportionate bandwidth allocation in randomly connected dilute networks with fixed connectivity in the limit of large  $\epsilon$ . Consider a randomly connected network with balanced resources (i.e.  $\sum_i \Lambda_i^0 = 0$ ) with  $N$  nodes and each node has a fixed connectivity  $d_i = K$ . Due to the homogeneity, the message  $a_{ij}$  in Eq. (12) are all equal to

$$a = 1 + \frac{1}{(K-1)a^{-1}} \Rightarrow a = \frac{K-1}{K-2}. \quad (41)$$

The message  $\tilde{y}_{ij}$  is given by

$$\tilde{y}_{ij} = \frac{\Lambda_j + \sum_{k \in \partial j \setminus i} \tilde{y}_{jk}}{K-1}. \quad (42)$$

For a resource balanced network, we have  $\langle \tilde{y}_{ij} \rangle = 0$  and we can obtain  $\langle \tilde{y}_{ij}^2 \rangle$  by squaring both sides and averaging Eq. (42), assuming that the branches are uncorrelated in the tree approximation,

$$\langle \tilde{y}_{ij}^2 \rangle = \frac{\langle \Lambda^2 \rangle}{(K-1)(K-2)}. \quad (43)$$

For the full current flow distribution, we have  $\langle y_{ij} \rangle = 0$  and

$$\sigma_y^2 = \langle y_{ij}^2 \rangle = \left\langle \left( \frac{a_{ij} \tilde{y}_{ij} - a_{ji} \tilde{y}_{ji}}{a_{ij} + a_{ji} - 1} \right)^2 \right\rangle = \frac{2(K-1)\langle \Lambda^2 \rangle}{K^2(K-2)}. \quad (44)$$

Similarly, we can obtain the mean and the variance of the flow fluctuations in closed form expressions by using the cavity method. Consider the resource fluctuations follow Gaussian distribution with mean equal to 0 and

$\langle \delta \Lambda_i^2 \rangle = \alpha^2 \langle \Lambda_i^2 \rangle$ , where  $\alpha$  is a parameter, then the flow fluctuations will also follow a Gaussian distribution with mean 0 and variance

$$\sigma_{\delta y}^2 = \frac{2(K-1)\langle \delta \Lambda^2 \rangle}{K^2(K-2)} = \alpha^2 \sigma_y^2. \quad (45)$$

To study the performance of the bandwidth allocation scheme, we express the overload probability and the excess current in a link  $(ij)$  as a function of  $\Delta L_{ij}$ . The overload probability of a link  $(ij)$  is given by

$$P_O^{(ij)} = \int_{\Delta L_{ij}/\sigma_{\delta y}}^{\infty} Dz = H\left(\frac{L_{ij}}{\sigma_{\delta y}}\right), \quad (46)$$

where  $Dz \equiv \frac{1}{\sqrt{2\pi}} \exp\left(-\frac{z^2}{2}\right) dz$  and  $H(x) \equiv \int_x^{\infty} Dz$ . For the excess current in a link  $(ij)$ , we have

$$P_C^{(ij)} = \int_{\Delta L_{ij}/\sigma_{\delta y}}^{\infty} Dz (z\sigma_{\delta y} - \Delta L_{ij}). \quad (47)$$

Consider the asymptotic behavior of the proportionate bandwidth allocation (i.e.  $\Delta L_{ij} = \epsilon |y_{ij}|$ ) in the limit of  $\epsilon \gg 1$ . The average overload probability is given by

$$P_O^{prop} = 4 \int_0^{\infty} Dy_0 \int_0^{\infty} Dy H\left(\frac{\epsilon \sigma_y y_0}{\sigma_{\delta y} y}\right). \quad (48)$$

Interchanging the order of integration of  $y_0$  and  $y$ ,

$$P_O^{prop} = \frac{2}{\pi} \int_0^{\infty} Dy \tan^{-1}\left(\frac{\alpha y}{\epsilon}\right). \quad (49)$$

For  $\epsilon \gg 1$ , we have

$$P_O^{prop} \approx \frac{2\alpha}{\pi\epsilon} \int_0^{\infty} Dy y = \sqrt{\frac{2}{\pi^3}} \frac{\alpha}{\epsilon}. \quad (50)$$

For the average excess current using the proportionate bandwidth allocation scheme, we obtain

$$P_C^{prop} = 4 \int_0^{\infty} Dy_0 \int_0^{\infty} Dy \int_{\epsilon y_0/\alpha y}^{\infty} Dz (\sigma_{\delta y} y z - \epsilon \sigma_y y_0). \quad (51)$$

To simplify the calculation, we interchange the order of the integration

$$P_C^{prop} = 4\sigma_y \int_0^{\infty} Dy \alpha y \int_0^{\infty} Dy_0 \int_{\epsilon y_0/\alpha y}^{\infty} Dz \left(z - \frac{\epsilon y_0}{\alpha y}\right). \quad (52)$$

By transforming to polar coordinates in the space of  $y_0$  and  $z$ , one can obtain

$$P_C^{prop} = \sigma_y \sqrt{\frac{2}{\pi}} \int_0^{\infty} Dy \frac{\alpha^2 y^2}{\sqrt{\alpha^2 y^2 + \epsilon^2 + \epsilon}}. \quad (53)$$

In the limit of  $\epsilon \gg 1$ , the above expression can be simplified as

$$P_C^{prop} = \frac{\alpha^2 \sigma_y}{2\epsilon} \sqrt{\frac{2}{\pi}} \int_0^{\infty} Dy y^2 = \frac{\alpha^2 \sigma_y}{\sqrt{8\pi\epsilon}}. \quad (54)$$

We further study the asymptotic behavior of the *minlink* algorithm in which  $\Delta L_{ij}$  is given by Eq. (34). To study the asymptotic behavior for large  $\epsilon$ , we express  $1/\lambda$  in terms of  $\epsilon$ . From the constraint Eq. (33), we have

$$2 \int_0^{\frac{1}{\lambda\sqrt{2\pi\sigma_{\delta y}}}} Dy \sigma_{\delta y} y \sqrt{2 \ln \left( \frac{1}{\lambda\sqrt{2\pi\sigma_{\delta y}} y} \right)} = 2\epsilon \int_0^{\infty} Dz \sigma_y z. \quad (55)$$

In the limit  $\epsilon \gg 1$ , it reduces to

$$\begin{aligned} 2\sigma_{\delta y} \int_0^{\infty} Dy y \sqrt{2 \ln \left( \frac{1}{\lambda\sqrt{2\pi\sigma_{\delta y}} y} \right)} &\approx \epsilon \sigma_y \sqrt{2/\pi} \\ \Rightarrow \frac{1}{\lambda} &\approx \sqrt{2\pi\sigma_{\delta y}} \exp \left( -\frac{\epsilon^2}{2\alpha^2} \right). \end{aligned} \quad (56)$$

The average overload probability using the *minlink* algorithm is given by

$$\begin{aligned} P_O^{link} &= 2 \int_{\frac{1}{\lambda\sqrt{2\pi\sigma_{\delta y}}}}^{\infty} Dy H(0) \\ &+ 2 \int_0^{\frac{1}{\lambda\sqrt{2\pi\sigma_{\delta y}}}} Dy H \left( \sqrt{2 \ln \left( \frac{1}{\lambda\sqrt{2\pi\sigma_{\delta y}} y} \right)} \right) \end{aligned} \quad (57)$$

In the limit  $\epsilon \gg 1$ , the sum is dominated by the second term. Using the approximation  $H(x) \approx \exp(-x^2/2)/(\sqrt{2\pi}x)$  when  $x \gg 1$ , and neglecting loga-

rithmic terms, we have

$$P_O^{link} \approx \frac{\alpha}{\pi\epsilon} \exp \left( -\frac{\epsilon^2}{2\alpha^2} \right). \quad (58)$$

Similarly, for the average excess current in the limit of  $\epsilon \gg 1$ , we have

$$\begin{aligned} P_C^{link} &\approx 2 \int_0^{\infty} Dy \sigma_{\delta y} y \int_{\epsilon/\alpha}^{\infty} Dz \left( z - \frac{\epsilon}{\alpha} \right) \\ &\approx \frac{\sigma_{\delta y} \alpha}{\pi\epsilon} \exp \left( -\frac{\epsilon^2}{2\alpha^2} \right). \end{aligned} \quad (59)$$

Lastly, for the *minflow* algorithm ( $\Delta L_{ij}$  with the form of Eq. (37)), we can obtain the asymptotic behavior with a similar procedure as above. In the limit of  $\epsilon \gg 1$ , using the constraint Eq. (34), one can express  $\epsilon'$  in terms of  $\epsilon$  as

$$2 \int_0^{\infty} Dy \epsilon' \sigma_{\delta y} y = 2 \int_0^{\infty} Dy_0 \epsilon \sigma_y y_0 \Rightarrow \epsilon' = \frac{\epsilon}{\alpha}. \quad (60)$$

The average overload probability using *minflow* is given by

$$P_O^{flow} = 2 \int_0^{\infty} Dy H \left( \frac{\epsilon' \sigma_{\delta y} y}{\sigma_{\delta y} y} \right) = \frac{\alpha}{\sqrt{2\pi}\epsilon} \exp \left( -\frac{\epsilon^2}{2\alpha^2} \right), \quad (61)$$

and the average excess current is given by

$$\begin{aligned} P_C^{flow} &= 2 \int_0^{\infty} Dy \int_{\epsilon'}^{\infty} Dz (\sigma_{\delta y} y z - \epsilon' \sigma_{\delta y} y) \\ &\approx \frac{\sigma_{\delta y} \alpha}{\pi\epsilon} \exp \left( -\frac{\epsilon^2}{2\alpha^2} \right). \end{aligned} \quad (62)$$

- 
- [1] <http://www.nerc.com/dawg/database.html>. Information on electric systems disturbances in North America.
  - [2] Electricity Consumers Resource Council. The economic impacts of the august 2003 blackout. *Washington, DC*, 2004.
  - [3] Ying-Cheng Lai, Adilson E Motter, and Takashi Nishikawa. Attacks and cascades in complex networks. In *Complex networks*, pages 299–310. Springer, 2004.
  - [4] Yuri V Makarov, Viktor I Reshetov, Vladimir A Stroeve, and Nikolai I Voropai. Blackouts in north america and europe: Analysis and generalization. *Proc. IEEE St. Petersburg PowerTech 2005*, pages 1–7, 2005.
  - [5] Yang Yang, Takashi Nishikawa, and Adilson E Motter. Small vulnerable sets determine large network cascades in power grids. *Science*, 358(6365):eaan3184, 2017.
  - [6] Jichang Zhao, Daqing Li, Hillel Sanhedrai, Reuven Cohen, and Shlomo Havlin. Spatio-temporal propagation of cascading overload failures in spatially embedded networks. *Nature communications*, 7:10094, 2016.
  - [7] Hengdao Guo, Ciyan Zheng, Herbert Ho-Ching Iu, and Tyrone Fernando. A critical review of cascading failure analysis and modeling of power system. *Renewable and Sustainable Energy Reviews*, 80:9–22, 2017.
  - [8] Ian Dobson and David E Newman. Cascading blackout overall structure and some implications for sampling and mitigation. *International Journal of Electrical Power & Energy Systems*, 86:29–32, 2017.
  - [9] Hao-Ran Liu, Yan-Long Hu, Rong-Rong Yin, and Yu-Jing Deng. Cascading failure model of scale-free topology for avoiding node failure. *Neurocomputing*, 260:443–448, 2017.
  - [10] Alberto Azzolin, Leonardo Dueñas-Osorio, Francesco Cadin, and Enrico Zio. Electrical and topological drivers of the cascading failure dynamics in power transmission networks. *Reliability Engineering & System Safety*, 175:196–206, 2018.
  - [11] Daniel Bienstock, Michael Chertkov, and Sean Harnett. Chance-constrained optimal power flow: Risk-aware network control under uncertainty. *SIAM Review*, 56(3):461–495, 2014.
  - [12] Mert Korkali, Jason G Veneman, Brian F Tivnan, James P Bagrow, and Paul DH Hines. Reducing cascading failure risk by increasing infrastructure network interdependence. *Scientific reports*, 7:44499, 2017.
  - [13] Zhen Shao and Haijun Zhou. Optimal transportation network with concave cost functions: loop analysis and

- algorithms. *Physical Review E*, 75(6):066112, 2007.
- [14] K.Y. Michael Wong and David Saad. Inference and optimization of real edges on sparse graphs: A statistical physics perspective. *Physical Review E*, 76(1):011115, 2007.
- [15] Dimitri P Bertsekas. *Linear network optimization: algorithms and codes*. MIT Press, 1991.
- [16] Chi Ho Yeung and David Saad. Networking: A statistical physics perspective. *Journal of Physics A: Mathematical and Theoretical*, 46(10):103001, 2013.
- [17] David J Thouless, Philip W Anderson, and Robert G Palmer. Solution of 'solvable model of a spin glass'. *Philosophical Magazine*, 35(3):593–601, 1977.
- [18] Marc Mézard, Giorgio Parisi, and Miguel Virasoro. *Spin glass theory and beyond: An Introduction to the Replica Method and Its Applications*. World Scientific Publishing Company, 1987.
- [19] K.Y. Michael Wong and David Saad. Equilibration through local information exchange in networks. *Physical Review E*, 74(1):010104, 2006.
- [20] E. Harrison, D. Saad, and K. Y. M. Wong. *Int. J. of Smart Grid and Clean Energy*, 2016.
- [21] Dominik Heide, Mirko Schäfer, and Martin Greiner. Robustness of networks against fluctuation-induced cascading failures. *Physical Review E*, 77(5):056103, 2008.
- [22] Réka Albert, Hawoong Jeong, and Albert-László Barabási. Attack and error tolerance of complex networks. *Nature*, 406(6794):378–382, 2000.
- [23] Adilson E Motter and Ying-Cheng Lai. Cascade-based attacks on complex networks. *Physical Review E*, 66(6):065102, 2002.
- [24] Paolo Crucitti, Vito Latora, and Massimo Marchiori. Model for cascading failures in complex networks. *Physical Review E*, 69(4):045104, 2004.
- [25] Mirko Schäfer, Jan Scholz, and Martin Greiner. Proactive robustness control of heterogeneously loaded networks. *Physical Review Letters*, 96(10):108701, 2006.
- [26] Ping Li, B-H Wang, Han Sun, Pan Gao, and Tao Zhou. A limited resource model of fault-tolerant capability against cascading failure of complex network. *The European Physical Journal B*, 62(1):101–104, 2008.
- [27] Steffen Bohn and Marcelo O Magnasco. Structure, scaling, and phase transition in the optimal transport network. *Physical Review Letters*, 98(8):088702, 2007.
- [28] Chi Ho Yeung, David Saad, and KY Michael Wong. From the physics of interacting polymers to optimizing routes on the london underground. *Proceedings of the National Academy of Sciences*, 110(34):13717–13722, 2013.
- [29] Judea Pearl. *Probabilistic reasoning in intelligent systems: networks of plausible inference*. Elsevier, 2014.
- [30] Yair Weiss. Correctness of local probability propagation in graphical models with loops. *Neural computation*, 12(1):1–41, 2000.
- [31] Peter G Doyle and J Laurie Snell. Random walks and electric networks, mathematical association of america, 1984. *arXiv preprint math.PR/0001057*.
- [32] C. H. Yeung and K. Y. Michael Wong. Optimal location of sources in transportation networks. *Journal of Statistical Mechanics: Theory and Experiment*, 2010(04):P04017, 2010.
- [33] Fan Chung and S.-T. Yau. Discrete green's functions. *Journal of Combinatorial Theory, Series A*, 91(1):191–214, 2000.
- [34] Allen J. Wood and Bruce F Wollenberg. *Power Generation, Operation, and Control*. John Wiley & Sons, 2012.
- [35] Cliff Grigg, Peter Wong, Paul Albrecht, Ron Allan, Murty Bhavaraju, Roy Billinton, Quan Chen, Clement Fong, Suheil Haddad, Sastry Kuruganty, et al. The iee reliability test system-1996. a report prepared by the reliability test system task force of the application of probability methods subcommittee. *IEEE Transactions on power systems*, 14(3):1010–1020, 1999.
- [36] Daniel Bienstock. Optimal control of cascading power grid failures. In *2011 50th IEEE Conference on Decision and Control and European Control Conference*, pages 2166–2173. IEEE, 2011.
- [37] Stephen Boyd and Lieven Vandenberghe. *Convex optimization*. Cambridge university press, 2004.
- [38] Jonathan S Yedidia, William T Freeman, and Yair Weiss. Constructing free-energy approximations and generalized belief propagation algorithms. *IEEE Transactions on Information Theory*, 51(7):2282–2312, 2005.